Performance of UWB SSMA Using Orthogonal PPM-TH over Dense Multipath Channels

Fernando Ramírez-Mireles
email:ramirezm@ieee.org
Instituto Tecnológico Autónomo de México (ITAM)
Río Hondo 1, Col. Tizapán San Angel,
México City, D.F. C.P. 01000,
México

Submitted November 2006

Abstract

In this work we study ultra wideband (UWB) communications over dense multipath channels using orthogonal pulse position modulation (PPM) for data modulation and time-hopping (TH) for code modulation. We consider the effects of the multiple access interference (MUI) in asynchronous spread spectrum multiple access (SSMA) based on random TH codes. We use a realistic multipath channel to analyze the effects of the transmission rate in the number of users for different bit error rate (BER) values.

Keywords: Ultra wideband communications, pulse position modulation, multipath channels, spread spectrum multiple access.

1 Introduction

The UWB communications for short-range high-speed wireless communications has been studied extensively [1]-[9]. This work studies the performance of binary UWB communications in the presence of additive white Gaussian noise (AWGN), MUI, and dense multipath effects (DME). Several authors have studied this problem before.

The work in [10] studied an *all-digital* receiver using time hopping with binary pulse amplitude modulation and synchronous time-division duplexing, with a multipath channel model that assumes the path arrival times being uniformly distributed over the delay spread span and the amplitude of each path being Gaussian decaying linearly with delay, and with the maximum delay spread fixed to a certain constant value.

The work in [11] studied a *digital* receiver using TH combined with orthogonal binary PPM including *multi-stage block-spreading* to cancel MUI deterministically, with the channel modeled with a finite impulse response filter of fixed

order that includes asynchronisms in the form of delay factors and frequency selective multipath effects.

The work in [12] used a signal-to-interference analysis to study the degradation factor due to MUI in the presence of DME when using binary PPM-TH signals, with a multipath model assuming path arrival times uniformly distributed over one frame period with special cases of exponentially decaying and flat amplitude profiles.

In [13] the error probability of UWB SSMA using TH combined with binary PPM is studied in the presence of interference and multipath, comparing performance for different modulation schemes, interference conditions, and receivers types.

In [14] a closed-form expression of the MUI variance in multipath channel for binary pulse amplitude modulation and time hopping PAM-TH was found.

In this work we use a simple expression for the BER [15] and consider a realistic multipath indoor office channel using the Time Domain Corporation Indoor Channel Database to analyze the effects of the transmission rate in the number of users for different BER values.

2 System Model

2.1 Transmitted Signals

The *transmitted* signal is described by

$$\Psi_{\text{TX}}^{(\nu)}(t) = \sum_{k=0}^{N_s-1} p_{\text{TX}}(t - kT_f - c_k^{(\nu)}T_c - b_j\delta) \,, \tag{1}$$

where t denotes time, the index k is the number of time hops that the signal $\Psi_{\text{TX}}^{(\nu)}(t)$ has experienced, T_f is the average frame time between pulse transmissions, and $p_{\text{TX}}(t)$ is the UWB pulse used to build the transmitted PPM signals.

The superscript $1 \leq \nu \leq N_u$, indicates user-dependent quantities, Without loss of generality, we will assume that user one is the desired user.

The b_j is the j^{th} data bit, $j = 1, 2$, taking one of two equally likely values from the binary set $\{0, 1\}$. The time shift value δ is chosen such that set of signals are orthogonal in the absence of multipath.

For a given time shift parameter T_c, the pseudo-random TH code $\{c_k^{(\nu)}\}$ provides an additional time shift to the pulse in every frame, each time shift being a discrete time value $c_k^{(\nu)}T_c$, with $0 \leq c_k^{(\nu)}T_c < N_hT_c$. The data bit changes only every N_s hops, i.e., the system uses fast time hopping.

The UWB pulse $p_{\text{TX}}(t)$ is the basic signal used to convey information. This pulse is characterized by a radiated spectrum with a very wide bandwidth (a few Giga Hertz) around a relatively low center frequency (one or two Gigahertz). The duration of the pulse T_p is in the order of a few nanoseconds.

As defined by the Federal Communications Commission (FCC) of the United States, any signal is of UWB nature when it has a 10 dB bandwidth of at least

500 MHz, or when its fractional bandwidth (the ratio of the 10 dB bandwidth to the central frequency) is at least 20 percent [16].

2.2 Model for the Gaussian Channel

Under free space propagation conditions the received signal

$$\Psi^{(\nu)}(t) = \sum_{k=0}^{N_s-1} p(t - kT_f - c_k^{(\nu)} T_c - b_j \delta) \tag{2}$$

is modeled as the derivative of the transmitted signal $\Psi_{\text{TX}}^{(\nu)}(t)$. This model for the antenna system has been repeatedly used [1]-[9]. Most existing UWB antennas do not have the differentiation effect. Even for those antennas systems, the analysis in this work still can be applied because it is based on the energy and correlation values of the *received* signals.

The received signal is modified by amplitude A_o and delay τ_o factors that depend on the transmitter-receiver separation distance (in our analysis we will assume $A_o = 1$ and $\tau_o = 0$).

The signals $\Psi^{(\nu)}(t)$ in (2) have duration $T_s = N_s T_f$ and energy

$$E_\Psi \triangleq \int_{-\infty}^{\infty} [\Psi^{(\nu)}(t)]^2 dt = N_s E_p \ , \tag{3}$$

for $j = 1, 2$, where $E_p = \int_{-\infty}^{\infty} [p(t)]^2 dt$ is the energy of the *received* UWB pulse $p(t)$. The signals $\Psi^{(\nu)}(t)$ have normalized correlation values

$$\beta \triangleq \frac{\int_{-\infty}^{\infty} \Psi_{j_1}^{(\nu)}(t)\, \Psi_{j_2}^{(\nu)}(t)\, dt}{E_\Psi} = \begin{cases} 1, & j_1 = j_2 \ , \\ \gamma(\delta), & j_1 \neq j_2 \ , \end{cases} \tag{4}$$

where

$$\gamma(\delta) \triangleq \frac{\int_{-\infty}^{\infty} p(t)\, p(t-\delta)\, dt}{E_p} \tag{5}$$

is the normalized autocorrelation function of $p(t)$. The time shift value $\delta = 2T_p$ is chosen such that the signal correlation $\gamma(\delta) = 0$.

The noise at the receiver's input $n(t)$ is AWGN with two-sided power spectrum density (PSD) $N_o/2$.

2.3 Model for the Multipath Channel

2.3.1 Multiple-Path Trajectories

For each active link the corresponding transmitter stays fixed at certain arbitrary position, and the corresponding receiver moves in a spatially random fashion.

In particular, the link between user one's receiver and user ν's transmitter defines a multiple-path propagation trajectory that is a function of the relative

position of user one's receiver with respect to the position of user ν's transmitter. This random trajectory will be identified with the random index $\xi^{(\nu)}$. There will be N_u of such trajectories, one for every pair (user ν's transmitter, user one receiver), $\nu = 1, 2, \ldots, N_u$.

When user ν's transmitter radiates the signal $p_{\text{TX}}(t)$, the signal detected by user one's receiver will be represented by $p(\xi^{(\nu)}, t)$. As we move user one's receiver position, these trajectories change. Hence, the received waveforms coming from each of the transmitters also change.

2.3.2 Channel Effect in the UWB Pulse

In an indoor multipath channel, transmission of the pulse $p_{\text{TX}}(t)$ results in a received "pulse" $\sqrt{E_a}\, p(\xi^{(\nu)}, t)$ which is is a multipath spread version of $p(t)$. The average duration of $p(\xi^{(\nu)}, t)$ is denoted T_a, and can be in the order of up to a few hundreds of nanosecond, hence $T_a >> T_p$. We will assume that T_a is the equivalent of the mean delay spread of the channel.

The pulse $\sqrt{E_a}\, p(\xi^{(1)}, t)$ has random energy $E_p(\xi^{(1)}) \stackrel{\triangle}{=} E_a\, \alpha^2(\xi^{(1)})$, where E_a is the average received energy, and $\alpha^2(\xi^{(1)}) \stackrel{\triangle}{=} \int_{-\infty}^{\infty} [p(\xi^{(1)}, t)]^2 dt$ is the normalized random energy. The pulse has normalized random signal correlation

$$\gamma(\xi^{(1)}, \delta) \stackrel{\triangle}{=} \frac{\int_{-\infty}^{\infty} p(\xi^{(1)}, t)\, p(\xi^{(1)}, t - \delta)\, dt}{\alpha^2(\xi^{(1)})} \ .$$

The normalized signal cross-correlation corresponding to pulses received with two different trajectories $\xi^{(1)}$ and $\xi^{(\nu)}$ is

$$\tilde{\gamma}(\xi^{(1)}, \xi^{(\nu)}, \delta) \stackrel{\triangle}{=} \frac{\int_{-\infty}^{\infty} p(\xi^{(1)}, t)\, p(\xi^{(\nu)}, t - \delta)\, dt}{\tilde{\alpha}^2(\xi^{(1)}, \xi^{(\nu)})} \ ,$$

where $\tilde{\alpha}^2(\xi^{(1)}, \xi^{(\nu)}) \stackrel{\triangle}{=} \int_{-\infty}^{\infty} p(\xi^{(1)}, t)\, p(\xi^{(\nu)}, t)\, dt$.

2.4 Model for the Multipath Channel

The PPM-TH signals received in the presence of multipath are

$$\Psi^{(\nu)}(\xi^{(\nu)}, t) = \sum_{k=0}^{N_s - 1} \sqrt{E_a} p(\xi^{(\nu)}, t - kT_f - c_k^{(\nu)} T_c - b_j \delta) \ . \tag{6}$$

The signal in (6) is received with trajectory $\xi^{(\nu)}$, and is a multipath spread version of the signal in (2).

Here we have assumed that the channel is slowly time invariant, therefore the PPM signal is composed of shifted version of the same spreaded pulse. We will further assume that $\Psi^{(\nu)}(\xi^{(\nu)}, t)$ has fixed duration $T_s \simeq N_s T_f$.

The signals $\Psi^{(1)}(\xi^{(1)}, t)$ have random energy

$$E_\Psi(\xi^{(1)}) \quad = \quad \int_{-\infty}^{\infty} [\Psi^{(1)}(\xi^{(1)}, t)]^2 dt \simeq \overline{E}_s \alpha^2(\xi^{(1)}), \tag{7}$$

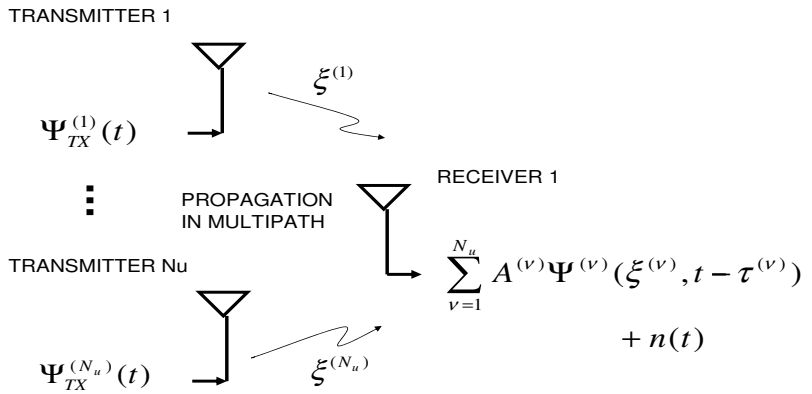

Figure 1: The case with multiple users.

where $\overline{E}_s = N_s E_a$ is the average bit energy. The signals have normalized random correlation values

$$\beta(\xi^{(1)}) \triangleq \frac{\int_{-\infty}^{\infty} \Psi_{j_1}^{(1)}(\xi^{(1)}, t)\, \Psi_{j_2}^{(1)}(\xi^{(1)}, t)\, dt}{E_\Psi(\xi^{(1)})} = \begin{cases} 1, & j_1 = j_2\ , \\ \gamma(\xi^{(1)}, \delta), & j_1 \neq j_2\ , \end{cases} \quad (8)$$

2.5 The Case with Multiple Users

Fig. 1 shows the system model under consideration, in which all the users transmit the same type of binary time hopping PPM signals in (1) to convey information, the difference being the TH code used for each user. Also, all the users experience the same multipath environment, although each one has its own multipath trajectory. When N_u asynchronous transmitters are active, the received signal at user one's receiver position is modeled as

$$r(t) = \sum_{\nu=1}^{N_u} A^{(\nu)} \Psi^{(\nu)}(\xi^{(\nu)}, t - \tau^{(\nu)}) + n(t)\ , \quad (9)$$

where $\tau^{(\nu)}$ represent time asynchronisms between the clock of user ν's transmitter and user one's receiver, $(A^{(\nu)})^2$ is the ratio of average power used by user ν's transmitter with respect to the average power used by user one's transmitter (with $(A^{(1)})^2 = 1$), and $n(t)$ represents non MUI interference modeled as AWGN.

The signal $r(t)$ in (9) is a random process that depends on the random noise $n(t)$ and three other types of random variables: The random time delays, denoted by the vector $\underline{\tau} = (\tau^{(2)}, \tau^{(3)}, \ldots, \tau^{(N_u)})$; the random time hopping codes, denoted by the vector $\underline{C} = (C^{(2)}, C^{(3)}, \ldots, C^{(N_u)})$, where each code $C^{(\nu)} = \{c_k^{(\nu)}\}$ for $k = 0, 1, \ldots, N_s - 1$; and the random multiple-path trajectories indexes, denoted by $\xi^{(1)}$ and the vector $\underline{\xi} = (\xi^{(2)}, \xi^{(3)}, \ldots, \xi^{(\nu)})$. Performance computation is based on signal-to-interference (SIR) ratios and BER rates averaged over all random variables.

To facilitate our analytical treatment, the following assumptions are made

1. The statistical behavior of the multipath channel depends only on the relative position of the receiver with respect to the transmitter. Hence, we treat $\xi^{(\nu)}$, $\nu = 1, 2, \ldots, N_u$, as independent, identically distributed (i.i.d.) uniform random variables.

2. Given that $\xi^{(\nu)}$, $\nu = 1, 2, \ldots, N_u$, are i.i.d., it follows that the expected values $\mathbf{E}_{\xi^{(\nu)}}\{\cdot\} = \mathbf{E}_{\xi^{(1)}}\{\cdot\}$ and $\mathbf{E}_{(\xi^{(1)}, \xi^{(\nu)})}\{\cdot\} = \mathbf{E}_{\xi^{(1)}}\{\mathbf{E}_{(\xi^{(\nu)}|\xi^{(1)})}\{\cdot\}\}$ are all the same for all ν, where $\mathbf{E}_{\xi^{(1)}}\{\cdot\}$ is the expected value operator with respect to $\xi^{(1)}$. As in [17], the expected values with respect to $\xi^{(\nu)}$ can be approximated with sample averages based on parameters calculated using measured or synthesized received waveforms.

3. We consider $p(\xi^{(\nu)}, t)$ with $\int_{-\infty}^{\infty} p(\xi^{(\nu)}, t)dt \simeq 0$.

4. In this work we assume that the channel is slowly time invariant. We don't consider the individual multipath components but the complete received waveform. Also, the receiver is able to perfectly match user one's received signal, i.e., $p(\xi^{(1)}, t)$ is perfectly estimated.

5. Since $\delta << T_f$ we will assume that in the MUI correlation terms $\delta = 0$ for $\nu = 1, 2, 3, \ldots, N_u$.

6. The elements $\{c_k^{(\nu)}\}$ for $\nu = 1, 2, \ldots, N_u$, and for $k = 0, 1, 2, \ldots, N_s - 1$, are i.i.d. random variables. Each $c_k^{(\nu)}$ is uniformly distributed on the interval $[0, N_h]$. We don't specify N_h because the assumption 8) produces results independent of it.

7. The transmission time differences $\tau^{(\nu)} - \tau^{(1)} \stackrel{\triangle}{=} \Phi^{(\nu)} T_f + \phi^{(\nu)}$, for $\nu = 2, \ldots, N_u$, are i.i.d. random variables, with $\phi^{(\nu)} \stackrel{\triangle}{=} \tau^{(\nu)} - \tau^{(1)} \bmod T_f$ being uniformly distributed on $[-T_f/2, T_f/2]$, where mod means the modulus operation. We don't characterize $\Phi^{(\nu)}$ because results are independent of it.

8. To avoid overlapping of pulses belonging to different frames in (1) the maximum time shift produced by the time hopping code is limited to $N_h T_c < ((T_f - T_a)/2) - \epsilon$, where $\epsilon \stackrel{\triangle}{=} 2(T_p + \delta)$. Combining this condition,

together with $T_f > (T_a+\epsilon)$, we can ensure that both inter-pulse and inter-symbol interference can be neglected. Even when inter-pulse interference is not negligible, for large N_s inter-symbol interference can be neglected.

9. We will assume that for each of the $N_u - 1$ MUI contributors the cross-correlation between signal terms belonging to different frames is much smaller than correlation of MUI within the same frame.

10. Cross-correlation between paths belonging to different fingers in the Rake receiver is taken into account.

11. We assume that power control can track and compensate large scale fading variations (perfect average power control). Hence, this analysis deals with small scale fading variations.

With these assumptions the net effect of the multiple access interference at the output of the demodulation circuit can be modeled as a zero mean Gaussian random variable (r.v.).

3 Validation of the Gaussian assumption

For the case under study, i.e., signals with several pulses per bit N_s, the Gaussian approximation for the effect of the MUI at the output of the correlator is justified by the central limit theorem for various users N_u. In this section we test the Gaussianity of the multiple access component y_m of the decision variable y by estimating the entropy of a sample of y_m as proposed in [18]. If the sample entropy is high enough, we consider the sample to be generated by a Gaussian source. For this purpose we use the following hypothesis testing

$$\text{Test(sample)} = \begin{cases} \text{Sample is Gaussian,} & \text{if } K_{nm} \geq K^* \\ \text{Sample is not Gaussian,} & \text{if } K_{nm} < K^*, \end{cases} \tag{10}$$

where

$$K_{nm} = \frac{n}{2m\overline{\sigma}} \left\{ \prod_{i=1}^{n} \left(\varrho_{(i+m)} - \varrho_{(i-m)} \right) \right\}^{1/n}, \tag{11}$$

is a normalized *Gaussianity index*, and where $\overline{\sigma}^2 \neq 0$, is the sample variance, n is the number of samples taken, $0 < m < n/2$ is a natural number, and $\varrho_{m(i+m)}$ are order statistics (samples of y_m): $\varrho_{(1)} \leq \varrho_{(2)} \leq .... \leq \varrho_{(n)}$. Notice that the quantity $\varrho_{(i+m)} - \varrho_{(i-m)}$ should be replaced by $\varrho_{(i+m)} - \varrho_{(1)}$ or $\varrho_{(n)} - \varrho_{(i-m)}$ when $i - m < 1$ or $i + m > n$, respectively.

The work in [19] showed that the point estimator K_{nm} is consistent with $\log_n(H)$, where H is the *true* entropy of the sample, i.e., K_{nm} converges in probability to $\log_n(H)$ when $n \to \infty$, $m \to \infty$, but $\frac{m}{n} \to 0$. The value $K^* = 3.35$ gives a 95 % confidence level for $n = 50$ and $m = 5$ [19].

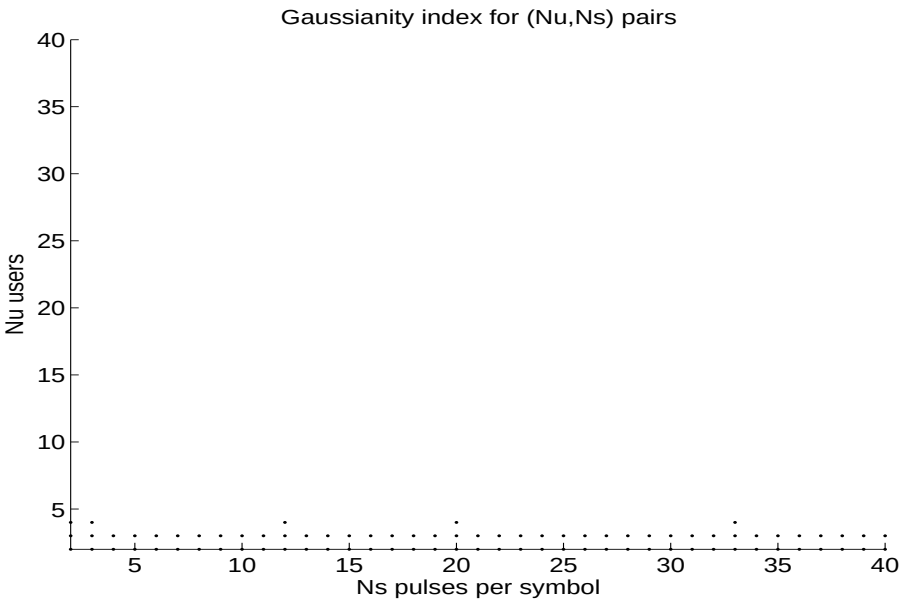

Figure 2: Gaussianity index: The dots in the plane denote the pairs (N_u, N_s) for which $K_{nm} \geq K^*$ for the first time.

Fig. 2 shows a plot with a plane consisting of pairs (N_u, N_s). The dots in the plane denote the pairs (N_u, N_s) for which $K_{nm} \geq K^*$ for the first time as N_u is increased for a fixed N_s, for different sample realizations. This figure shows that indeed, for any number of pulses per symbol N_s, we need a low number of users n_u to consider the MUI as Gaussian.

4 Receiver Signal Processing and Performance

To simplify notation, in the following analysis we will drop the super-index $^{(1)}$ from $\Psi^{(1)}(\xi^{(1)}, t)$, $A^{(1)}$, $\tau^{(1)}$, and $c^{(1)}$.

4.1 Signal Detection

Let's assume that the receiver wants to demodulate user one's signal. The received signal $r(t)$ in (9) can be rewritten

$$r(t) \quad = \quad A\Psi(\xi, t-\tau) + n_{\text{TOT}}(t),\ t \in \mathcal{T}\ , \tag{12}$$

where $\mathcal{T} \triangleq [\tau, N_s T_f + \tau]$, and

$$n_{\text{TOT}}(t) \triangleq \sum_{\nu=2}^{N_u} A^{(\nu)} \Psi^{(\nu)}(\xi^{(\nu)}, t-\tau^{(\nu)}) + n(t)\ .$$

For the time being, let's assume that user one's receiver is static at one place, and that user one's transmitter is at a fixed position, i.e., ξ is kept fixed.

In the present analysis signal detection is achieved using a Rake receiver [20]. For binary communications a perfectly synchronized rake Receiver will have 2 filters matched to $\Psi_j(\xi, t-\tau)$, $j = 1, 2$. The output of the j^{th} matched filter

$$y_j \quad = \quad \int_{t\in\mathcal{T}} r(t)\ \Psi_j(\xi, t-\tau)dt \stackrel{\triangle}{=} y_s + y_m + y_n\ , \tag{13}$$

can be seen as the sum of three outputs: the output y_s of a filter perfectly matched and synchronized to the signal, the output y_m of a filter mismatched and asynchronous to the interference, and the output y_s consisting of filtered noise.

The signal term y_s takes into account the correlation of the desired user with itself

$$y_s \quad = \quad \int_{t\in\mathcal{T}} A\ \Psi(\xi, t-\tau)\ \Psi_j(\xi, t-\tau)dt = \begin{cases} E_\Psi(\xi), & \text{for } \Psi(\cdot) = \Psi_j(\cdot)\ , \\ E_\Psi(\xi)\ \beta(\xi), & \text{for } \Psi(\cdot) \neq \Psi_j(\cdot)\ , \end{cases} \tag{14}$$

The multiple-access term y_m takes into account the cross-correlation among user one and the interfering users

$$\begin{aligned} y_m \quad &= \quad \int_{t\in\mathcal{T}} \sum_{\nu=2}^{N_u} A^{(\nu)}\ \Psi^{(\nu)}(\xi^{(\nu)}, t-\tau^{(\nu)})\ \Psi_j(\xi, t-\tau)\ dt \\ &= \quad \sum_{\nu=2}^{N_u} \sum_{k=0}^{N_s-1} A^{(\nu)} E_a \tilde{\alpha}^2(\xi, \xi^{(\nu)}, \tau^{(\nu)}) \tilde{\gamma}(\xi, \xi^{(\nu)}, \Omega_k^{(\nu)} - \phi^{(\nu)} - (b_{j_1} - b_j)\delta), \end{aligned} \tag{15}$$

where $\Omega_k^{(\nu)} \stackrel{\triangle}{=} c_{k-\Phi^{(\nu)}}^{(\nu)} - c_k$.

Finally, the noise term is

$$y_n = \int_{t\in\mathcal{T}} n(t)\ \Psi_j(\xi, t-\tau)\ dt\ . \tag{16}$$

4.2 Performance Conditioned on ξ

The performance of the correlation receiver can be analyzed using traditional detection theory [21] (since the MUI is modeled as Gaussian noise, this correlation receiver is sub-optimum, the optimum receiver being a multi-user detector [22]). The demodulation problem can be analyzed as the time-shift-coherent detection of M equal-energy, equally-likely signals in the presence of Gaussian interference plus noise using a binary correlation receiver. The resulting performance results should be considered as a lower bound, i.e., performance of an ideal Rake receiver.

The BER is given by

$$\mathrm{UBPe}(N_u|\xi) = \int_{\sqrt{\mathrm{SIR}_{\mathrm{out}}(N_u|\xi)}}^{\infty} \frac{\exp(-\rho^2/2)}{\sqrt{2\pi}}\, d\rho, \tag{17}$$

where

$$\mathrm{SIR}_{\mathrm{out}}(N_u|\xi) \;\triangleq\; \frac{1}{\left[\mathrm{SIR}_{\mathrm{out}}(1|\xi)\right]^{-1}+\left[\mathrm{SIR}_{\mathrm{MUI}}(N_u|\xi)\right]^{-1}}\,, \tag{18}$$

is the output bit SIR observed in the presence of $N_u - 1$ other users and, for the time being, is being conditioned on ξ. The

$$\mathrm{SIR}_{\mathrm{out}}(1|\xi) \;\triangleq\; \frac{E_s\,\alpha^2(\xi)\,[1-\beta(\xi)]}{N_o} \tag{19}$$

is the bit SNR in the presence of AWGN and in the absence of MUI, and

$$\mathrm{SIR}_{\mathrm{MUI}}(N_u|\xi) \;\triangleq\; \frac{E_s\,\alpha^2(\xi)\,[1-\beta(\xi)]}{N_{\mathrm{MUI}}(\xi)} \simeq \frac{\mathcal{G}(\xi)}{N_u}\,, \tag{20}$$

is the bit SNR in the presence of MUI and in the absence of AWGN, where $N_{\mathrm{MUI}}(\xi)$ is the *equivalent* PSD level of the total MUI, and where $\mathcal{G}(\xi) \triangleq \frac{\mu(\xi)/T_f}{R_b}$ is a *random* processing gain factor, where $R_b = 1/T_s$ is the bit transmission rate, and where

$$\mu(\xi) \;=\; \frac{m_p^2(\xi,\xi,0,0,\delta)}{\mathbf{E}_{(\xi^{(\nu)}|\xi)}\{\int_{-\infty}^{\infty} m_p^2(\xi,\xi^{(\nu)},\varsigma,0,\delta)\,d\varsigma\}} \tag{21}$$

is a normalized random SIR parameter defined in terms of both the received UWB pulse shape and the time-shift defining the orthogonal PPM data modulation, where $\mathbf{E}_{(\xi^{(\nu)}|\xi)}\{\cdot\}$ is the expected value with respect to $\xi^{(\nu)}$ conditioned on ξ, and where

$$\begin{aligned} m_p(\xi,\xi^{(\nu)},\varsigma,0,\delta) \;&\triangleq\; \int_{-\infty}^{\infty} p(\xi^{(\nu)},\varrho)\;[p(\xi,\varrho)-p(\xi,\varrho-\delta)]\,d\varrho \\ &= \begin{cases} \alpha^2(\xi)\times \\ \quad[\gamma(\xi,\varsigma)-\gamma(\xi,\varsigma-\delta)]\,, & \text{for } \nu=1\,, \\ \tilde{\alpha}^2(\xi,\xi^{(\nu)})\times \\ \quad\left[\tilde{\gamma}(\xi,\xi^{(\nu)},\varsigma)-\tilde{\gamma}(\xi,\xi^{(\nu)},\varsigma-\delta)\right]\,, & \text{for } \nu\neq 1\,. \end{cases} \end{aligned} \tag{22}$$

The averaged performance can be obtained by taking the expected value $\mathbf{E}_\xi\{\cdot\}$ of (17) over all values of ξ to get

$$\overline{\mathrm{UBPe}}\left(\frac{\overline{E}_s}{N_o}, N_u\right) \;=\; \mathbf{E}_\xi\{\mathrm{UBPe}\,(N_u|\xi)\}\,. \tag{23}$$

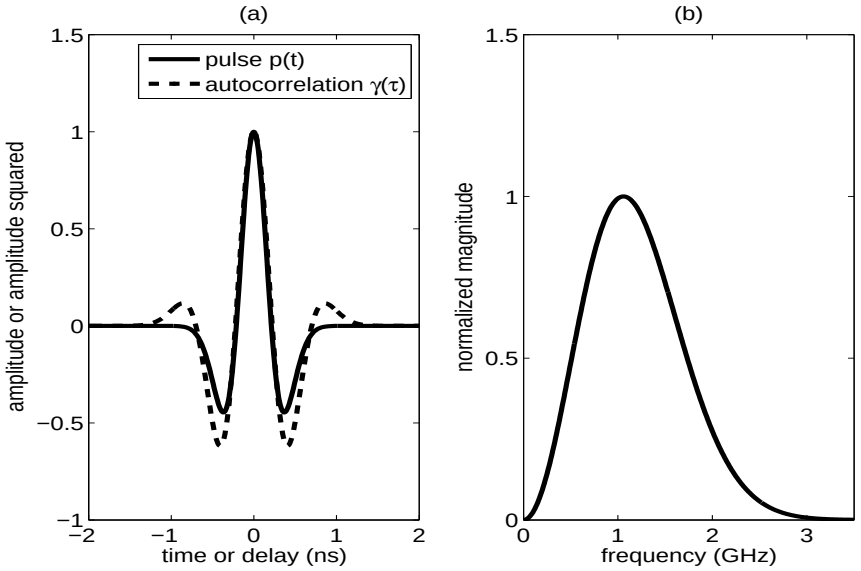

Figure 3: The plots for (a) $p(t)$ and $\gamma(\tau)$, and (b) the spectrum of $p(t)$

5 Numerical Results

5.1 UWB Pulse

In this numerical example the UWB pulse is the second derivative of a Gaussian pulse

$$p(t) = \left[1 - 4\pi \left[\frac{t}{t_n}\right]^2\right] \exp\left(-2\pi \left[\frac{t}{t_n}\right]^2\right), \tag{24}$$

for $-T_p/2 \leq t \leq T_p/2$, where t_n is a parameter that determine the pulse duration. The pulse energy $E_p = 3t_n/8$. For this pulse the signal correlation function is

$$\gamma(\tau) = \left[1 - 4\pi \left[\frac{\tau}{t_n}\right]^2 + \frac{4\pi^2}{3}\left[\frac{\tau}{t_n}\right]^4\right] \exp\left(-\pi \left[\frac{\tau}{t_n}\right]^2\right), \tag{25}$$

for $-T_p \leq \tau \leq T_p$.

For $t_n = 0.7531$ ns we get a pulse duration $T_p \simeq 2.0$ ns. In this case the spectrum of $p(t)$ is centered at about 1.1 GHz, with a 3 dB bandwidth of about 1.2 GHz, easily satisfying the traditional definition of UWB signal stating that the 10 dB bandwidth of the signal should be at least 20 percent of its center frequency [16]. Fig. 3 shows this pulse.

The set of $p(\xi^{(\nu)}, t)$ were taken from the Time Domain Corporation Indoor Channel Database, available at USC's ULTRA-LAB WEB site at *http* :

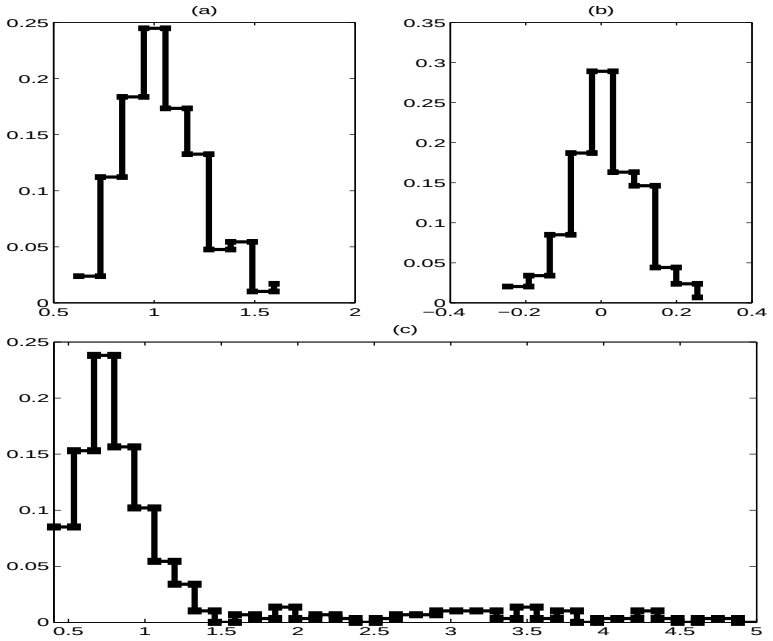

Figure 4: The histograms for (a) $\alpha^2(\xi)$, (b) $\beta(\xi)$, and (c) $\mu(\xi)$. The ordinate represents appearance frequency, and the abscissa represents the value of the parameter.

//click.usc.edu/New _Site/database.html. These UWB "pulses" have an average delay spread $T_a \simeq 300$ ns.

5.2 Calculations

For this example we use $T_f = 350$ ns and $R_b = 100$ to $R_b = 1000$ kilobits per second (Kbps) per user. For the Gaussian case we use $\alpha^2 = 1$ and $\beta = 0$ and calculate $\mu \simeq 1.3$. Similar to [17], the calculations for the multipath case are based on sample averages over the different realizations of $\alpha^2(\xi)$, $\beta(\xi)$ and $\mu(\xi)$ considering a sample size of 49 for every room, and averaging the results over 5 rooms. Fig. 4 depicts histograms for $\alpha^2(\xi)$, $\beta(\xi)$ and $\mu(\xi)$.

Fig. 5(a) shows BER vs. Nu for $R_b = 100, 500, 1000$ kbps. Fig. 5(b) shows the number of users Nu to preserve a BER value for $R_b = 100$ to 1000 Kbps.

6 Conclusions.

In this work we study UWB SSMA communications over multipath channels based on PPM-TH. We analyze the effects of the transmission rate in the number of users for different BER.

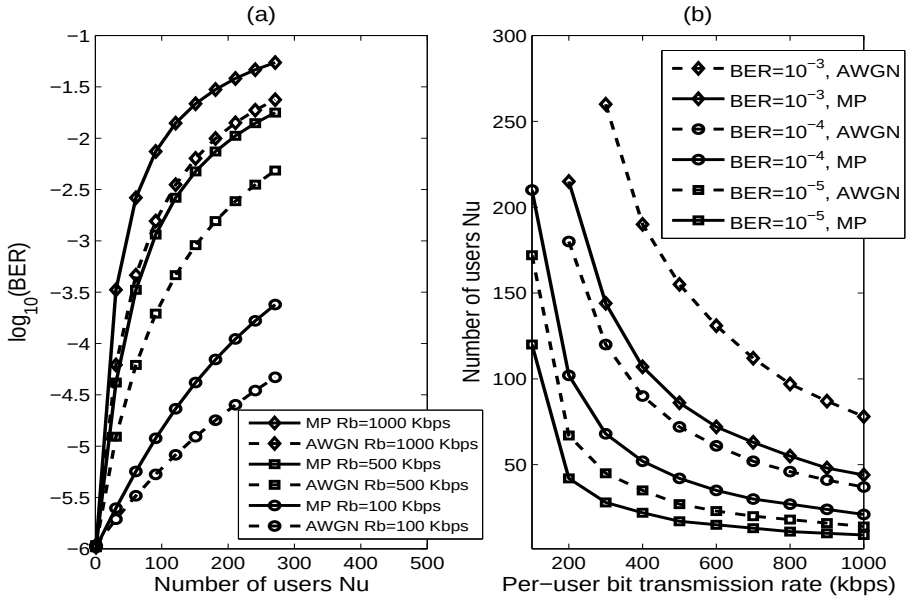

Figure 5: (a) BER vs. number of users for different R_b. (b) Number of users to preserve BER for a given R_b

Fig. 5(b) shows the number of users Nu to preserve a BER value for different values of R_b in Kbps. For the BER and SIR values in Fig. 5(a), $\mathrm{SIR}_{\mathrm{MUI}}(N_u|\xi)$ dominates over $\mathrm{SIR}_{\mathrm{out}}(1|\xi)$ and therefore $N_u \simeq \frac{1}{\mathrm{SIR}_{\mathrm{out}}(N_u|\xi)} \frac{\mu(\xi)/T_f}{R_b}$.

For the type of signals and indoor office channel under consideration, these result indicate the following:

- For BER=10^{-5}, e.g., in data applications requiring low BER, the number of simultaneous radio links decreases from more than 100 to less than 10 when R_b goes from 100 kbps to 1000 kbps. This corresponds to a decrease in a factor in the order of 10 in the processing gain.

- For BER=10^{-3}, e.g., in voice applications supporting high BER, the number of simultaneous radio links decreases from more than 200 to less than 50 when R_b goes from 300 kbps to 1000 kbps. This corresponds to a decrease in a factor in the order of 3.4 in the processing gain.

- To obtain a combination with $N_u \geq 100$ users, $R_b \geq 1$ Megabits per second, and BER$\leq 10^{-5}$, some form of forward error correction must be used.

References

[1] R. A. Scholtz, Multiple Access with Time Hopping Impulse Modulation, invited paper, in Proc. IEEE MILCOM Conf. (1993), pp. 447-450.

[2] P. Withington II and L. W. Fullerton, An Impulse Radio Communications System, in Ultra-Wideband, Short-Pulse Electromagnetics, H. L. Bertoni, L. Carin and L. B. Felson, Ed. New York: Plenum Press (1993), pp. 113-120.

[3] F. Ramrez-Mireles, M. Win, and R. Scholtz, Performance of Ultra-WideBand Time-Shift-Modulated Signals in the Indoor Wireless Impulse Radio Channel, in Proc. 31st Asilomar Conf. on Signals, Systems, and Computers, vol. 1 (1997), pp. 192-196.

[4] Special issue on ultra-wideband radio in multiaccess wireless communications, IEEE J. Select. Areas Commun., vol. 20, no. 9 (2002).

[5] Special issue on UWB - State of the art, EURASIP JASP., vol. 2005, no. 3 (2005).

[6] Special issue on UWB wireless communications - A new horizon, IEEE Trans. on Veh. Tech., vol. 54, no. 5 (2005).

[7] Special issue: Ultra wideband for wireless communications, Wireless Communications and Mobile Computing, vol. 5, no. 5 (Aug 2005).

[8] Special issue on ultra-wideband communications, IEEE J. Select. Areas Commun., vol. 24, no. 4, Part 1 (2006).

[9] R. C. Qiu, H. Liu, X. Shen,, Ultra-Wideband for Multiple Access Communications, in IEEE Commun. Magazine, Vol. 43, No. 2 (2005), pp. 2-8.

[10] C.J. Le Martret and G.B. Giannakis, All-Digital PAM Impulse Radio for Multiple-Access Through Frequency-Selective Multipath, in Proc. IEEE GLOBECOM Conf. (2000), pp. 77-81.

[11] L Yang and G.B. Giannakis, Impulse Radio Multiple Access Through ISI Channels with Multi-Stage Block-Spreading, in Proc. IEEE UWBST Conf. (2002), pp. 277-282.

[12] A. Taha and K. M. Chugg, Multipath Diversity Reception of Wireless Multiple Access Time-Hopping Digital Impulse Radio, in Proc. IEEE UWBST Conf. (2002), pp. 283-288.

[13] G. Durisi et al, A General Method for Error Probability Computation of UWB Systems for Indoor Multiuser Communications, in Journal of Communications and Networks, Vol. 5, no. 4 (2003), pp. 354-364.

[14] C. J. Le Martret, A-L Deleuze, P. Ciblat, Optimal time-hopping Codes for multi-user interference mitigation in ultra-wide bandwidth impulse radio, in IEEE Trans. on Wireless Commun., vol. 5, no. 6 (2006), pp. 1516-1525.

[15] F. Ramírez-Mireles, Error Probability of Ultra Wideband SSMA in a Dense Multipath Environment, in Proc. IEEE MILCOM Conf., Vol. 2 (2002), pp. 1081 - 1084.

[16] U.S. Federal Communications Commission, First Report and Order for UWB Technology, U.S. Federal Communications Commission, April 2002.

[17] F. Ramírez-Mireles, On Performance of Ultra Wideband Signals in Gaussian Noise and Dense Multipath, IEEE Trans. Veh. Technol., Vol. 50, no.1 (2001), pp. 244-249.

[18] F. Ramírez-Mireles and A. Almada, An Entropy-Based Gaussianity Test for Pulse-Based UWB MUI With Perfect and Imperfect Power Control, submitted to IEEE Trans. on Veh. Technol.

[19] Vasicek Oldrich, A Test for Normality Based on sample Entropy, Journal of the Royal Statistical Society Series B, vol. 38, No. 1 (1976), pp. 54-59.

[20] J. G. Proakis, Digital Communications, New York:McGraw-Hill (1995).

[21] R. M. Gagliardi, Introduction to Telecommunications Engineering, John Wiley and Sons (1988).

[22] E. Fishler and H. V. Poor, Low-Complexity Multiuser Detectors for Time-Hopping Impulse-Radio Systems, IEEE Trans. on Signal Processing, Vol. 52, no. 9 (2004), pp. 2561-2571.